shown in Fig. 1(e). After etching to 300 nm deep, the rms roughness of the surface increased from 1 nm to 3 nm as measured using the phase shift interference mode of the optical profilometer.

The NEXAFS measurements were undertaken in the range 280-305 eV (C K-edge) in partial electron yield mode with an electron analyzer energy of 165 eV, for which the mean free path of Auger electrons, and thus the surface sensitivity, corresponds to a few (<5) atomic layers. A rectangular area 430 µm x 200 µm wide was etched to match the expected spot size of the synchrotron beam. The etch depth was 50 nm. An ablated 500 µm rectangular grid was placed around the etched area to enable the etched surface to be conveniently located in the NEXAFS spectrometer. The NEXAFS spectrum for the etched surface is presented in Fig. 5 (blue curve). The bulk x-ray absorption edge occurs at 289 eV, with the observation of a strong C 1s core-hole exciton resonance. The pre-edge region contains information on unoccupied surface electronic states within the band gap. Two clear features of differing origin are observed. Feature A is associated with sp^2 hybridized carbon [18,21]. The spectrum for freshly cleaved highly oriented pyrolytic graphite (also included in Fig. 5) clearly shows the peak energy and magnitude corresponding to a graphite surface. The small sp^2 signal appearing in the spectrum of the etched surface is not attributed to generation of etching-induced sp^2 but due to slight overlap of the x-ray beam with the graphite-containing locating grid as confirmed by comparison with the spectrum of the virgin surface containing an ablated grid of twice the density (red curve). Feature B is associated with oxygen termination and in particular the 'top' bonded (ketone) oxygen [22]. The similar areas of B in the etched and un-etched spectra indicate no major change in the level of 'top' bonded oxygen termination between the initial chemically oxidized surface and the laser etched one.

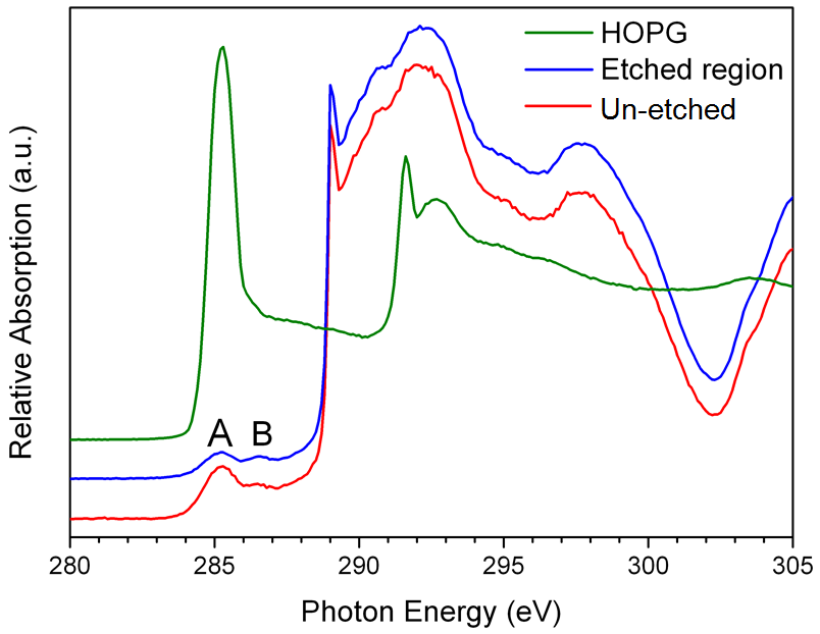

Fig. 5. NEXAFS spectrum for the laser etched surface compared with spectra for high oriented pyrolitic graphite (HOPG) and the un-etched surface. Feature A indicates sp^2 hybridized carbon which appears in the etched and un-etched spectra due to presence of graphite containing locator grids.

3. Discussion

The observed etch rate and surface analysis of the treated surface allow us to make the following conclusions about the etching process:

#149550 - $15.00 USD Received 21 Jun 2011; revised 4 Jul 2011; accepted 4 Jul 2011; published 12 Jul 2011

1. Etching is observed at pulse fluences and peak powers at least two orders of magnitude lower than characteristic fluences for ablation. The etch rate scales with approximately the square of intensity and this relationship is reproduced as a function of position on the surface in accordance with the incident beam profile.

2. The intrapulse etch rate, defined here as the etch depth per pulse divided by the pulse duration FWHM, has a similar dependence on pulse irradiance for ns and ps pulses. When plotted alongside the picosecond measurements of ref [16] (20 ps pulses at 78 MHz repetition rate) and the 248 nm results in ref [15] (15 ns pulses at 100 Hz) as shown in Fig. 6, it is evident that the intrapulse etch rates have a similar dependence on incident intensity suggesting that the rate is largely independent of pulse duration in the range 10^{-10} – 10^{-8} s and pulse repetition rate in the range 10^{2} - 10^{8} Hz. The I_p^2 dependence observed in this study reveals a proportional relationship between the energy absorbed by the two-photon process (proportional to $\beta I_p^2 \Delta t$ where β is the TPA coefficient and Δt is the pulse duration) and the number of ejected atoms. The etch rate for 15 ns pulses at 248 nm at pulse repetition rate <100 Hz [15] also shows similar dependence but at a systematically higher rate. The higher rate may partially result from the higher TPA coefficient for the shorter wavelength (β_{248} = 1.60 cm GW^{-1} and β_{266} = 1.48 cm GW^{-1} [17]), although this is not enough to completely explain the difference. The observed independence with pulse repetition rate from 78 MHz to less than 100 Hz is expected given that multi-pulse effects are unlikely to be significant due to the short relaxation time of free carriers and surface thermal gradients (less than a nanosecond [23,24]) compared to the interpulse period.

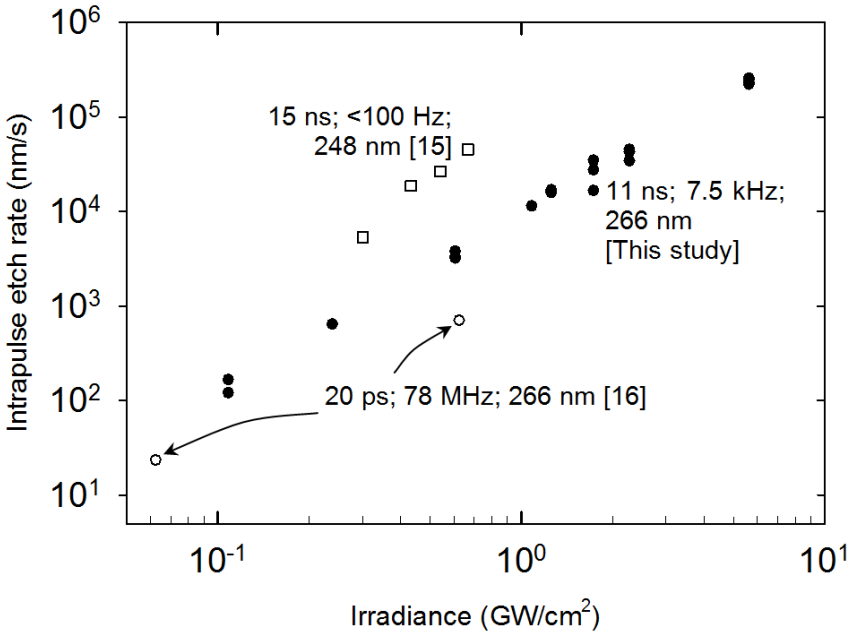

Fig. 6. Comparison of the intrapulse etch rate as a function of pulse irradiance (filled circles) with etching for 20 ps pulses at 266 nm and 78 MHz repetition rate reported in ref [16] (hollow circles) and for 15 ns pulses at 248 nm and pulse rate <100 Hz [15] (hollow squares).

3. The surface roughness increases from 1 nm to 3 nm upon etching to a depth of 300 nm. Low roughness is crucial in many applications, to reduce scattering losses in optical applications for example, and to improve device performance in electronics and MEMS. For waveguides in Si, scattering losses less than the order of the absorption losses are typically obtained for roughness values the order of 5-10 nm (see for

#149550 - $15.00 USD Received 21 Jun 2011; revised 4 Jul 2011; accepted 4 Jul 2011; published 12 Jul 2011

example [25]). Thus 2-photon etching is promising for creating a range of low scatter loss optical surfaces.

4. The etched surface is oxygen terminated and free from graphite. In contrast, graphite formation is intrinsic to laser ablation [11,17,26–28], and ablated features are often characterized by cracking, spalling, crater-halo and debris [28,29]. Although ultrafast machining has enabled reduced formation of graphite [17], and improved resolution [17,30], the absence of graphite in the etched surface observed herein is crucial to enabling linear cumulative etching (as shown in Fig. 2) and an advantage for avoiding post processing (such as ozone, plasma, annealing or chemical treatments).

5. Etching is found to proceed at rates largely independent of the facet direction. We observe etch rates for [100] and polycrystalline surfaces within approximately 20% (as shown in Fig. 2). Etching was also reported [16] for Brewster angled surfaces (63.7 degrees from [110]) at rates similar to the present study when taking into consideration the shorter pulse duration (see Fig. 6). We have also undertaken preliminary etching investigations of polished [110] surfaces which suggest that etching also proceeds at a rate similar to that seen for other surfaces.

These observations reveal that UV etching of diamond in air is a promising and highly versatile method for slow and controlled removal of surface atoms. The most striking observation is the I_p^2 dependence of the etch rate over a large range of pulse durations and pulse rates. Such a well-defined etch rate dependence spanning 3 orders of magnitude, which has not been seen in any other material as far as we are aware, is indicative of a mechanism of particle ejection that is a direct consequence of TPA. TPA by the surface atoms and in the bulk needs to be considered. We discount TPA in the air adjacent the surface due to the small cross-section for TPA in any major air constituents and due to the weak influence on etch rate we observe in the pressure range 1-1000 mb. Kononenko *et al* deduced that thermal processes were too small to account for any observed enhancement of surface oxidation and proposed that surface oxidation was mediated by electron-hole recombination in the diamond bulk [15]. At room temperature, electron hole pairs in diamond form Wannier-Mott excitons with binding energy 80 meV and potential energy just below the indirect band gap [31]. These excitons may diffuse to the surface and give up the stored energy (5.2 eV) to break surface bonds. The exciton energy is sufficient to desorb CO from [100] surfaces, for example, which has an activation energy of desorption of 1.67 eV [32]. If exciton decay at the surface is the dominant cause of desorption, the diffusion length of excitons will be a crucial parameter determining the etching rate and the minimum spatial resolution of etched structures. One would expect that the minimum feature size would be comparable to, or longer than, the diffusion length L_{ex}. Our results suggest that L_{ex} is less than a few microns to account for the observed diameter of the etch pit of less than 5 μm. An upper bound of 5 μm for L_{ex} was deduced on the basis of photo-electron emission yield measurements [33]. However, there seems to be some uncertainty in the value with other reports suggesting values from 200 nm [31] to 200 μm [34]. We note that if L_{ex} < 200 nm, the calculated probability for an exciton created by TPA within L_{ex} of the surface to eject a single carbon atom exceeds unity. If L_{ex} is longer than 5 μm, it may be necessary to consider absorption in the adsorbed oxygen layer to account for the sub-5 μm resolution observed herein.

A notable corollary of the two-photon desorption mechanism at sub-ablation fluences is that etching persists for very low UV fluences, and that even under incoherent illumination diamonds will steadily lose mass. However, the effect under ambient light conditions is rather insignificant. For example, continuous wave Hg lamp illumination at 253 nm for typical irradiances (0.1 W cm^{-2}) would require approximately 10^{10} years to desorb a significant mass (e.g. 1 μg) from a surface a few millimetres square. Under sunlight conditions the etching rate is even slower due to the reduced irradiance (10^{-4} W cm^{-2}; 300-350 nm) and the reduced probability for TPA at longer wavelengths. Of more practical significance, the I_p^2 dependence is of interest for enabling etching using methods other than laser direct-write and sources

#149550 - $15.00 USD Received 21 Jun 2011; revised 4 Jul 2011; accepted 4 Jul 2011; published 12 Jul 2011

other than Q-switched and ultrafast lasers. The field enhancement provided by wavelength scale probe structures (such as those used in scanning near field microscopy) can provide adequate etch rates at small pulse energies (eg., [35]). Projection of patterns using broad area mask imaging and interferometric methods are also interesting avenues for creating high resolution structures. Progress in AlGaN quantum well diode lasers emitting in the deep UV regime (see. e.g [36].) may lead to highly compact sources suitable for etching small areas. Depending on the aforementioned diffusion characteristics of the two-photon excited state, the combination of high resolution scanning methods and pulse fluences corresponding to near single atom removal rates may be an attractive and flexible technique for atomic removal from diamond surface atoms with near single atom precision.

In conclusion, etching of diamond in air is observed at etch rates 10^{-6}-10^{-3} nm/pulse using nanosecond pulses at 266 nm. The oxygen termination of the surface is preserved and free from sp^2 hybridized carbon and graphite. Carbon removal is proportional to TPA of the incident beam and occurs over a large range of fluences up to the ablation threshold. The absence of a threshold indicates substantial promise for enabling a wide range of high resolution structures using diverse techniques such as direct write processing, near-field, masking and interferometric illumination.

Acknowledgments

The authors thank Prof Vitaly Konov for interesting discussions on this subject, Adam Joyce, Carlo Bradac and Törsten Gaebel for their expert assistance in the surface profile analysis methods, and Dr Bruce Cowie for his expert assistance in performing the x-ray measurements. This material is based on research sponsored by the Australian Research Council Future Fellowship Scheme (FT0990622), and the Air Force Research Laboratory under agreement number AOARD-10-4078.